frontiers | Frontiers in Bioengineering and Biotechnology

TYPE Original Research
PUBLISHED 21 March 2025
DOI 10.3389/fbioe.2025.1530034

Check for updates

OPEN ACCESS

EDITED BY
Jesus Ortiz,
Italian Institute of Technology (IIT), Italy

REVIEWED BY
Wenxin Niu,
Tongji University, China
Jawad Masood,
Northwestern Metallurgical Research Association, Spain

*CORRESPONDENCE
Kaicheng Qi,
qkc@hebut.edu.cn

RECEIVED 18 November 2024
ACCEPTED 03 March 2025
PUBLISHED 21 March 2025

CITATION
Qi K, Yin Z, Li C, Zhang J and Song J (2025) Effects of a lumbar exoskeleton that provides two traction forces on spinal loading and muscles.
Front. Bioeng. Biotechnol. 13:1530034.
doi: 10.3389/fbioe.2025.1530034

COPYRIGHT
© 2025 Qi, Yin, Li, Zhang and Song. This is an open-access article distributed under the terms of the Creative Commons Attribution License (CC BY). The use, distribution or reproduction in other forums is permitted, provided the original author(s) and the copyright owner(s) are credited and that the original publication in this journal is cited, in accordance with accepted academic practice. No use, distribution or reproduction is permitted which does not comply with these terms.

Effects of a lumbar exoskeleton that provides two traction forces on spinal loading and muscles

Kaicheng Qi[1,2,3]*, Zhiyang Yin[1,2,3], Chao Li[1,2,3], Jianjun Zhang[1,2,3] and Jingke Song[1,2,3]

[1]School of Mechanical Engineering, Hebei University of Technology, Tianjin, China, [2]Hebei Provincial Key Laboratory of Robot Sensing and Human-Machine Integration, Tianjin, China, [3]Engineering Research Center of the Ministry of Education for Intelligent Rehabilitation Devices and Testing Technology, Tianjin, China

In workplaces with prolonged or repetitive stooping, disc herniation due to excessive pressure at the lumbar L5/S1 joints has been a difficult condition to prevent and treat in the field of lower back pain. Previous research on lumbar exoskeletons mainly focused on the impact of assistive torque on muscle activation, overlooking the fact that providing assistive torque is not the optimal approach when bending over with a low load. Instead, using traction force to reduce disc pressure is a more adaptable method to mitigate the risk of intervertebral disc herniation. In this paper, a novel lumbar exoskeleton mechanism is proposed. The exoskeleton principle is similar to a lever arranged on the torso, which provides two types of traction forces using a single compression spring with a lower support moment and higher traction performance. Subsequently, a kinetic simulation model covering passive physiologic tissues and spring stiffness was developed to determine the optimal range of traction forces for a given load, to predict the disc pressure and muscle activation at optimal traction forces. Eight subjects were invited to wear the exoskeleton for stooping and lifting tests under extreme loads, using myoelectric sensors to measure muscle activation. The results confirm that optimal traction force effectively reduces L5/S1 disc pressure without additionally increasing muscle activation. The exoskeleton in this study provides an alternative idea for the design of lumbar exoskeletons adapted to light load stooping.

KEYWORDS

lumbar exoskeleton, traction forces, intervertebral disc pressure, stiffness optimization, electromyography

1 Introduction

Lower back pain has been a significant factor in worker productivity in fields such as agriculture, manual labor, medical care, and manufacturing (Friedrich et al., 2000; Keawduangdee et al., 2012; D'ERRICO et al., 2013; Fethke et al., 2015). To reduce the risk of workers suffering from lower back pain, a range of active and passive exoskeletons have been developed and put into production (De Looze et al., 2016; Ali et al., 2021; Kranenborg et al., 2023).Active exoskeletons use motors as a drive source to provide sufficient power for the human, but active exoskeletons are structurally heavy and have a short range, workers are more likely to accept passive exoskeletons (Govaerts et al., 2024; Poliero et al., 2022).Currently, exoskeletons tend to assist stooping by generating extension

moments. If the moment curve is idealized, it can make the back muscles not to exert any force at all. Laevo, as a classic mass-produced industrial exoskeleton (Moya-Esteban et al., 2023; Luger et al., 2023; Hwang et al., 2021),is simple in structure and easy to wear. The exoskeleton is fitted with a cam-spring booster at the hip joint, which generates a supportive extension moment when the worker is stooping. The exoskeleton achieves a compact design that significantly reduces the size of the rigid booster mechanism, however, due to the size constraints of the cams, the exoskeleton requires an extremely high spring stiffness to generate an effective torque. The SPEXOR developed by Näf MB(Koopman et al., 2020b; Näf et al., 2018) has two elastic energy storage modules to generate torque, but the exoskeleton provides too much torque, which is more favorable in lifting situations above 15 kg. For low load bending, the excessive torque will severely interfere with the kinematics of the wearer's natural bending state, making it necessary for the user to change the movement strategy. Some flexible exoskeletons, such as the biomechanical garments represented by PLAD (Lamers et al., 2017; Abdoli-e and Stevenson, 2008; Abdoli-Eramaki et al., 2007; Frost et al., 2009), use stretchable bands to simulate the back muscles generating force along the tendons. Since the bands have a longer force arm, these exoskeletons have an advantage in reducing the activation of the lower back muscles.

Previous exoskeleton assistance mechanisms primarily aimed to augment human muscle force, with electromyography (EMG) testing often serving as a standard for evaluating exoskeleton performance (Moya-Esteban et al., 2023; Abdoli-E et al., 2006). However, spinal load is a crucial indicator of lumbar injury risk, and changes in kinematics or reductions in muscle force do not necessarily correspond to a decrease in spinal loads (Picchiotti et al., 2019; Madinei and Nussbaum, 2023; Koopman et al., 2020a). In reality, the body undergoes a "flexion-relaxation phenomenon" during stooping, a natural strategy to reduce energy expenditure. At a certain degree of lumbar flexion, passive tissues such as ligaments contribute the majority of the extension moments, leading to a "silent" phase in the active electromyographic signals of the erector spinae muscles (McGill and Kippers, 1994; Toussaint et al., 1995; Colloca and Hinrichs, 2005; Solomonow et al., 2003). At this stage, the body requires little external assisting moment and may be more sensitive to the moment demands of the exoskeleton. Therefore, the moment demands on the lumbar exoskeleton are not as great at this time. This situation is more likely to occur in low load stooping manual work such as agriculture or handicrafts rather than large object handling tasks. In that case, following a conventional exoskeleton would not be conducive to reducing L5/S1 spinal loading (Eskandari et al., 2025). A blanket reduction of active electrical signals from the muscles may not be optimal. In contrast, due to the shorter moment arm of the lumbar ligaments, there remains a risk of spinal loads (Toussaint et al., 1995). Excessive spinal load, which may lead to intervertebral disc injury, is a critical factor in evaluating lower back pain (Jaffar Nur and Abdol, 2017), yet it is often overlooked in exoskeleton design. Traction force can increase disc height, providing a mechanical effect that alleviates spinal pressure and mitigates disc herniation (Zaïri et al., 2021; Tadano et al., 2019; He et al., 2024; Chow et al., 2017; Pellecchia, 1994). However, exoskeletons capable of delivering tractional support are still yet to be developed. Chaerim Moon (Moon et al., 2022) proposed a lower back exoskeleton with a 4-bar linkage structure, using a tensile spring with a stiffness of 11,700 N/m to generate traction and extension torque. The system employs a tension sensor to estimate a traction force of approximately 100 N.

This paper makes the following contributions: 1) We propose a novel back exoskeleton that, unlike traditional designs which primarily generate moments to assist human motion, takes into account the flexion-relaxation phenomenon observed in lumbar passive tissues during flexion-extension movements. This exoskeleton respects the contributions of passive muscle force and ligaments in deep flexion. The exoskeleton mechanism is designed to enhance traction force at the expense of some extension moments. Theoretically, this conversion allows the exoskeleton to avoid impeding human movement, with the reduced extension moments minimizing the risk of abnormal abdominal muscle activation. From a biomechanical perspective, this exoskeleton is more adaptable to work environments involving frequent lifting tasks with light or zero loads. 2) We developed a dynamic simulation framework for the interaction between the human and the back exoskeleton. This framework identifies the optimal exoskeleton stiffness under 8 kg-load conditions, analyzing its combined effects on muscle coordination, spinal load, and muscle activation. The simulation is constrained to sagittal plane two-dimensional motion and passive exoskeleton mechanics (assuming all exoskeleton structures are lightweight, without affecting traction mechanics). Previous motion models often predicted movement trajectories as solutions to optimization problems, which could result in lumbar motion angles that do not accurately reflect natural human movement characteristics. In this study, we focus on how traction force in the back exoskeleton influences muscles and intervertebral discs during standard flexion-extension movements, with inverse dynamics optimization serving as the main direction of our research.

2 Exoskeleton design

2.1 Design overview

The back exoskeleton we designed has the same structure on the left and right sides of the body (Figure 1), with the overall structure symmetrically arranged along the sagittal plane. The exoskeleton mechanism resembles a lever placed on each side of the body. When the body bends forward, the compression spring gradually compresses, generating two equal but opposite spring forces. The upward spring force is applied to the chest pad, pulling the upper body upward; we refer to this as the chest traction force. The downward spring force is distributed at the A_3 point, acting as the driving force at the power point of the exoskeleton lever. The resistance force is distributed at the lever's resistance point A_4 on the back. If the back support rod is considered a two-force bar, an equal and opposite force is generated at the back pad position, directed upward along the back support rod; we call this the back traction force. The connection joint between the lever and the thigh support plate serves as the pivot point A_5, allowing the lever to reach a balanced state through the interactions of these elements. The reaction force at the pivot is transferred to the thigh support plate.

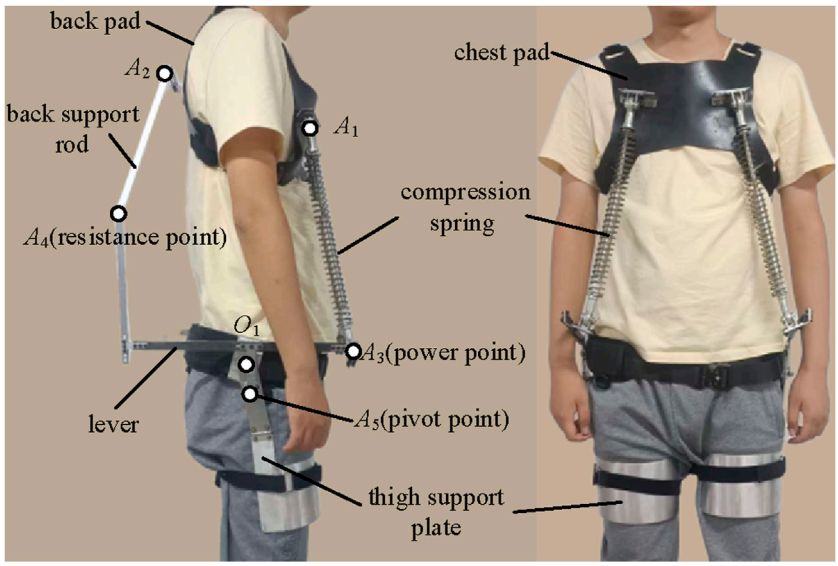

FIGURE 1
Scheme configuration of the exoskeleton side view. $A_4A_5A_3$ are connected to form a lever rod, with A_3 as the power point, A_4 as the resistance point, and A_5 as the lever pivot point. Chest traction force is directed along A_3A_1 and back traction force is directed along A_4A_2.

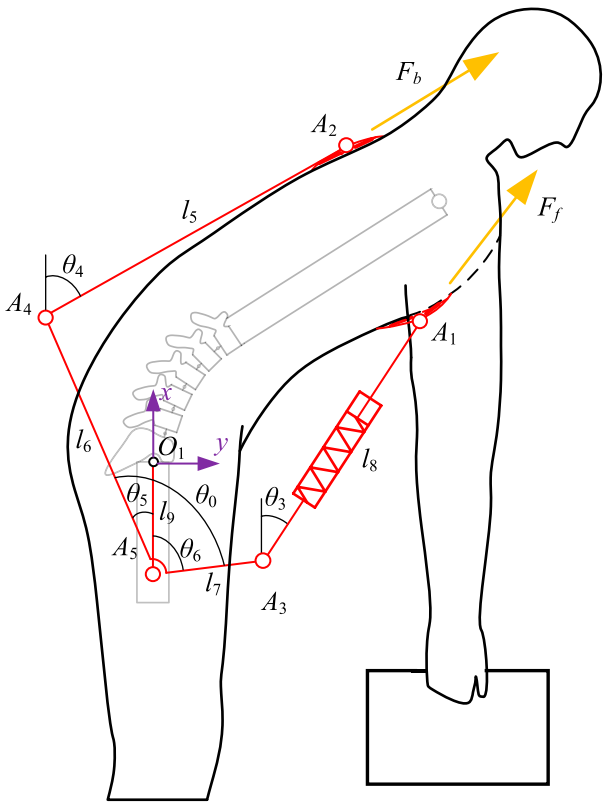

FIGURE 2
Sketch of the mechanism consisting of a human and an exoskeleton. The sketch simplifies the spinal part of the human body, defines the angles and dimensions of the exoskeleton used to solve the kinematics and traction forces, and labels the direction of the chest traction force F_f and the back traction force F_b.

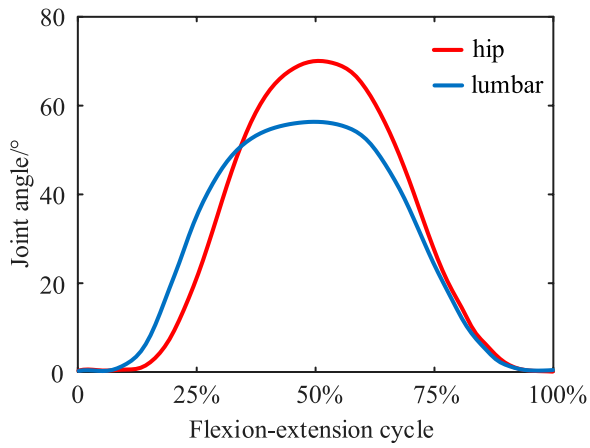

FIGURE 3
Synergistic movement patterns of the lumbar spine joints and hip joints during standard flexion and extension exercises.

2.2 Traction force model

A simplified sketch of the human-exoskeleton mechanism (Figure 2) allows to analyze the relationship between the upper body motion and the compression of the spring, with reference to the angles of the lumbar spine and hip joints under standard flexion-extension movements measured by Pal et al. (2007) (Figure 3), synergistic movement patterns of the vertebrae by Wong et al. (2006), to calculate the traction law generated by the exoskeleton under a standard flexion-extension cycle.

An absolute coordinate system is established at the hip joint O_1 (note: all angles are referenced to this coordinate system), then two

closed-loop vector equations are created to describe the mechanism motion (Equations 1, 2):

$$\begin{cases} x_{A_2} = l_6 \cos\theta_5 + l_5 \cos\theta_4 - l_9 \\ y_{A_2} = l_6 \sin\theta_5 + l_5 \sin\theta_4 \end{cases} \tag{1}$$

$$\begin{cases} x_{A_1} = l_7 \cos\theta_6 + l_8 \cos\theta_3 - l_9 \\ y_{A_1} = l_7 \sin\theta_6 + l_8 \sin\theta_3 \end{cases} \tag{2}$$

where (x_{A2}, y_{A2}) and (x_{A1}, y_{A1}) are the coordinates of point A_2, position of the exoskeleton tied to the back, and point A_1, position of the exoskeleton tied to the chest, respectively, in the absolute coordinate system. To simplify the model, the left and right limbs are assumed to be perfectly symmetrical during flexion and extension movements, so we model the human body as a multi-rigid linkage in the sagittal plane (Manns et al., 2017). Due to the limited range of independent motion of the head and thoracic spine relative to the lumbar spine (Consmüller et al., 2012), we treat them as a single rigid body. The lumbar region is represented as a sequentially articulated mechanism with five vertebrae and the pelvis connected by revolute joints. The elbow and wrist joint angles are fixed, and the arms are assumed to remain vertical throughout the flexion-extension process to simulate the natural hanging posture of the arms during bending and lifting. Since flexion primarily requires small joint angles at the knees and ankles (Bazrgari et al., 2007; Carnegie et al., 2022), the entire lower limb is treated as a rigid body fixed to the ground. Subsequent analyses will disregard the kinematic influence of the lower limbs on the human body and exoskeleton. The whole human body model consists of 8 rigid bodies including arms, thoracic vertebrae, lumbar vertebrae, sacrum, and thighs, with 6 degrees of freedom (lighter lines in Figure 2).

The geometric dimensions and inertia parameters of the vertebrae are based on measurements by Kuo et al. (2010), Pearsall et al. (1996). The coordinates of the points A_2, A_1 with the movement of the upper body were obtained using the homogeneous coordinate transformation method, after which the variation of the spring length could be calculated (Equations 3, 4):

$$\begin{cases} l_8 = \sqrt{\left(x_{A_1} + l_9 - l_7 \cos\theta_6\right)^2 + \left(y_{A_1} - l_7 \sin\theta_6\right)^2} \\ \theta_3 = \dfrac{y_{A_1} - l_7 \sin\theta_6}{x_{A_1} + l_9 - l_7 \cos\theta_6} \end{cases} \tag{3}$$

$$\begin{cases} \theta_5 = \arcsin\dfrac{h_0 \sin\varphi}{h_1} - \arccos\dfrac{h_1^2 + l_6^2 - l_5^2}{2h_1 l_6} \\ \theta_4 = \arcsin\dfrac{h_0 \sin\varphi - l_6 \sin\theta_5}{l_5} \\ \varphi = \arctan\dfrac{y_{A_2}}{x_{A_2}} \\ h_0 = \sqrt{x_{A_2}^2 + l_9^2 + y_{A_2}^2} \\ h_1 = \sqrt{h_0^2 + l_9^2 + 2h_0 l_9 \cos\varphi} \\ \theta_6 = \theta_0 + \theta_5 \end{cases} \tag{4}$$

Consider an ideal compression spring that, with damping and preload force neglected, produces a chest traction force (spring force) of (Equation 5):

$$F_f = k_s (l_{s0} - l_8) \tag{5}$$

where k_s is the sum of the spring stiffnesses of the exoskeleton on both sides and l_{s0} is the initial length of the spring of the human body in the standing phase. Assuming that the exoskeleton consists entirely of lightweight rods, we can derive the static equilibrium equations for the lever. This allows us to determine the mathematical relationship between the two types of traction forces (Equation 6):

$$F_b = \frac{F_f l_7 \sin(\theta_6 - \theta_3)}{l_6 \sin(\theta_5 + \theta_4)} \tag{6}$$

where F_b is the back traction force. The mathematical model predicts the trend of the two traction forces generated by the exoskeleton under standard flexion and extension movements.

The moments for the body due to chest and back traction are calculated by the cross-multiplication of the vectors from points A_1 and A_2 to the L5/S1 joints and the vectors of the chest and back traction forces, and the sum of the two moments is the total moment of the exoskeleton.

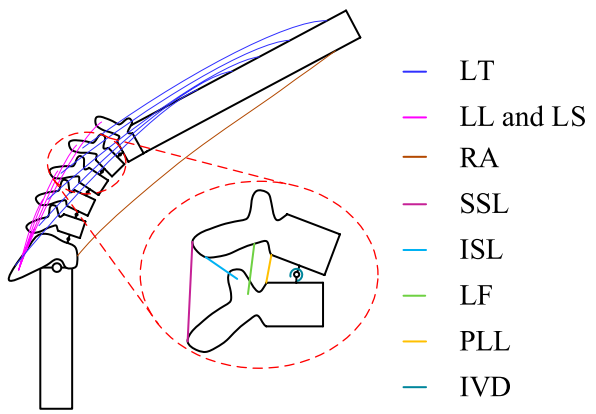

FIGURE 4
Schematic diagram of the tissues that make a major contribution during flexion-extension movements. It contains the distribution of the erector spinae muscle groups, the distribution of lumbar spine ligaments.

2.3 Stiffness optimization

According to the traction force model, there is a direct relationship between exoskeleton spring stiffness and traction force. The amount of traction force affects the body's muscle force generation. Too little traction force can lead to insufficient assistive effect, and the disc pressure will remain at a high threshold, which is not effective in avoiding spinal injuries. Too much traction force may lead to negative muscle activity, which in turn may cause injury to the human body. By establishing a musculoskeletal-based kinetic model, the effect of traction force on the musculoskeletal system under the phenomenon of flexion relaxation can be simulated, and the decompression performance of the exoskeleton with optimal traction force can be obtained.

Due to the complexity and large number of low back muscle groups, we simplify the calculations by modeling only the erector spinae muscle as the main force-generating muscle group in flexion and extension, with a total of 22 muscle fibers. Within this muscle group, muscle fiber bundles are divided into the thoracic

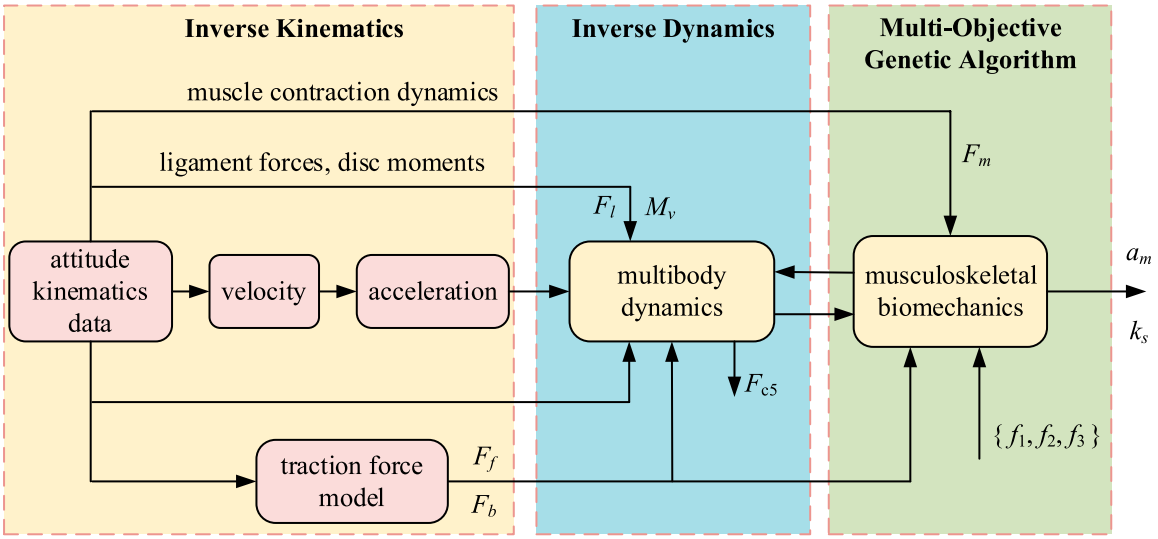

FIGURE 5
Simulation flow of spring stiffness and muscle activation level, an inverse dynamics calculation method. The simulation results show the optimized spring stiffness, the degree of muscle activation before and after the traction force is applied and the L5/S1 disc pressure.

longissimus (LT), lumbar iliocostalis (LL), and lumbar longissimus (LS) based on the different attachment points of the muscle fibers (Figure 4). In contrast, the rectus abdominis (RA) was also modeled to represent the antagonist muscle of the longest muscle of the thoracic spine. Muscle contraction dynamics are described using the hill model (Millard et al., 2013), expressed as follows (Equation 7):

$$F_m = F_{om}\left(a_m F_{am} + F_{pm}\right) \tag{7}$$

where, F_m is the total muscle force, F_{am} is the dominant force factor, F_{pm} is the passive force factor, F_{om} is the maximum isometric force of the muscle fiber, a_m is the muscle fiber activation.

The posterior longitudinal ligament (PLL), ligamentum flavum (LF), supraspinous ligament (SSL), and interspinous ligament (ISL), which play a primary role in the flexion-extension movement, were selected (Figure 4). The attachment points of these four lumbar spine ligaments on the vertebrae were determined according to the method described by Naserkhaki et al. (2018). The ligament stiffness data followed the force-deflection curves determined by Pintar et al. (1992) for ligaments of the lumbar T12-L2, L2-L4, and L4-Sl segments. For computational convenience, nonlinear stiffness curves for all ligaments were fitted with a sixth-degree polynomial, which when multiplied by the ligament stretch can be expressed as the ligament force F_l. The intervertebral disc joint was modeled as a torsion spring with constant stiffness in the coronal axis to calculate the disc's resistance moment M_v, and their stiffness data were obtained from (Senteler et al., 2016).

The Newton-Euler method was employed to establish the multi-body dynamics equations for each rigid body (Equation 8), which can visualize the contact forces between different vertebrae, as well as the contributions made by active and passive muscle forces, ligaments, and intervertebral discs to the generation of extension moments. This, in turn, facilitates the assessment of intervertebral disc pressures. The L5/S1 intervertebral disc pressure, which is a combination of disc moments, muscle forces, ligament forces, and vertebral joint forces F_x, F_y, can be written as:

$$F_{c5} = F\left(F_m, F_l, F_x, F_y, M_v\right) \tag{8}$$

Since the unknown amount of muscle fiber activation is much larger than the number of equations in the kinetic model, optimization algorithms are required to obtain solutions, while different objective functions lead to variability in the optimization results (Ostraich and Riemer, 2024). We formulate the muscle as well as the stiffness solution problem as a multi-objective optimization problem (Figure 5) with constraints based on the dynamical equations of Newton's Euler method and a range of muscle activation a_m. Considering that with a spring stiffness of 2000 N/m the exoskeleton traction force will be close to the effective traction force threshold of 500 N (Zaïri et al., 2021), the stiffness does not exceed this value. It is constructed as follows (Equations 9, 10):

$$min\ \ f\left(a_m, k_s\right) = \{f_1, f_2, f_3\} \tag{9}$$

$$s.t.\left\{\begin{array}{l} ma = \sum F_x + \sum F_y + \sum F_m + \sum F_l \\ J\ddot{\theta} = \sum F_x \times l_x + \sum F_y \times l_y + \sum F_m \times l_m + \sum F_l \times l_l + \sum M_v \end{array}\right\}$$
$$0 \le a_m \le 1 \tag{10}$$

where m represents the mass, J represents the rotational inertia, a represents the acceleration, and $\ddot{\theta}$ represents the angular acceleration of the joint. l_x, l_y, l_m, l_l are the force arms of each component of the force relative to the disc rotating the joint, respectively.

The first objective function is the minimization of the sum of squares of muscle activation (Equation 11), which means that the sum of work done by human muscles is minimized. It is widely applied in various muscle optimization solution problems (Rahmati et al., 2017; De Groote et al., 2016; Manns et al., 2017). Unlike other methods, the optimization values of muscle activation in this function are related to the corresponding maximal isometric

force, indicating that muscle fibers with greater force capacity will tend to exert more force.

$$f_1 = \sum_{i=1}^{22} \frac{200\left(a_{m,i}\right)^2}{F_{om,i}} \tag{11}$$

The second objective function employs the total sum of squared differences to minimize the variation in activation levels among all muscle fibers (Equation 12). This reflects the body's ability to neurally marshal muscle, with similarity in activation changes of muscle fibers that play the same role when muscle groups are stimulated through the same or approximate reflex pathway.

$$f_2 = \sum_{i=1}^{22} \sum_{j=i+1}^{22} \left(a_{m,i} - a_{m,j}\right)^2 \tag{12}$$

The third objective minimizes the cumulative reaction force and moment at the L5/S1 intervertebral disc over a flexion-extension cycle (Equation 13), with w_1, w_2 and w_3 representing weight coefficients, $F_{L5/S1}$, $M_{L5/S1}$, and M_{hip} representing the L5/S1 force, the L5/S1 moment, and the hip moment, respectively. This reflects the body's tendency to generate active muscle forces in a way that minimizes skeletal load (Brown and Potvin, 2005). Although the optimization principles of these three objective functions may conflict, they together capture the true activation patterns of the erector spinae muscles during bending and lifting movements. Including exoskeleton spring stiffness in the optimization framework does not shift the optimization direction; on the contrary, it represents an optimal stiffness that reduces spinal load and muscle activation without compromising muscle coordination.

$$f_3 = w_1\left\|F_{L5/S1}\right\| + w_2\left\|M_{L5/S1}\right\| + w_3\left\|M_{hip}\right\| \tag{13}$$

The simulation framework was constructed and executed in MATLAB 2022b, with optimization conducted using a multi-objective genetic algorithm (MOGA) (Deb, 1999). MOGA balances multiple objective functions by finding a set of non-dominated solutions (Pareto optimal solutions) to achieve the best compromise between different objectives. The L5/S1 intervertebral disc pressure before wearing the exoskeleton was solved by assigning the degree of muscle activation through a multi-objective genetic algorithm, so as to assign a reasonable muscle force to each joint to satisfy the equilibrium of kinetic states. The spring stiffness was optimized according to the peak pressure of L5/S1 joints, and the L5/S1 disc pressure after wearing the exoskeleton was optimized by incorporating the traction force. The simulation timestep was set to 0.1 s, with the model starting in an initial upright posture, bending to the lowest point, then returning to an upright stance, covering a total duration of 4 s. This setup allows the simulation to capture real-time loading on intervertebral discs and changes in activation levels across individual muscle fibers of the erector spinae. For ease of analysis, the muscle fibers were grouped into three major muscle groups—thoracic longissimus, lumbar iliocostalis and longissimus, and rectus abdominis. The activation level of each muscle group was represented by the sum of activations of the fibers within that group.

3 Experiment

3.1 Subjects and procedures

A total of eight healthy male subjects were invited to participate voluntarily in the trial, with a mean age of 24 ± 1.5 years, mean height of 176 ± 8.3 cm, and mean weight of 73.3 ± 5.8 kg. All subjects had no report of low back pain in the last 3 months and had not been involved in large lifting tasks. Before the experiment, all subjects read the instructions and precautions related to the experiment and signed an informed consent form for the experiment. The experiment was approved by the Ethical Review Committee of Hebei University of Technology.

Raw EMG data were recorded using a Noraxon Ultium Wireless Surface EMG Tester (Noraxon Inc., United States) with a sampling frequency of 2000 Hz. The skin of the subjects was shaved before the experiment, and then cleaned of grease and other contaminants by wiping with an alcohol cotton ball. The surface EMG sensors were attached to the thoracic erector spinae (TES), lumbar erector spinae (LES), and rectus abdominis (RA), of which the thoracic erector spinae and lumbar erector spinae were mainly responsible for trunk flexion and extension, and the rectus abdominis muscle was responsible for trunk flexion. Before the experiment, the sensor light was covered with black tape to prevent the motion capture system from misjudging it as a Marker point. The kinematic data of the joints were recorded using a Vicon T40-S Motion Capture System (Oxford Metrics Ltd., United Kingdom) with a sampling frequency of 200 Hz. Reflex point markers were attached to T7, T12, S1, PSIS, ASIS, hip, mid-thigh, knee, mid-calf, ankle, and tip of the foot. The angle of the vector formed between the labeled points was used as the angle of joint movement during the experiment.

3.2 Procedures

The experiment was divided into four groups: No weight in hands without exoskeleton, 8 kg weight in hands without exoskeleton, no weight in hands with exoskeleton, and 8 kg weight in hands with exoskeleton. During the complete experiment, subjects were asked to keep their arms parallel to the direction of gravity at all times. Without the exoskeleton, the subjects were bending from the initial standing position in a natural descending motion to the subjective conscious limit, and then returned to the standing position in a natural rising motion without artificial intervention of synergistic movements between lumbar vertebrae and hip joints. There is no artificial interference with the synergistic movement between the lumbar spine and the hip joints. The phases from standing to bending, and from rising to standing, were all approximately 2 s. The choice of 0 kg was made in view of the fact that even without a load, the disc pressure during bending is not optimistic, and back pain in farmers has been reported in the field of agricultural harvesting or cultivation (Fathallah, 2010). 8 kg was chosen because it is the load level at which the NOISH lifting criteria for L5/S1 disc compression can reach the injury risk threshold (McGill and Kippers, 1994).The two loads represent most of the typical light-duty load-bearing work situations. Subjects wore the exoskeleton and started the experiment with a bending and rising motion without the exoskeleton as the

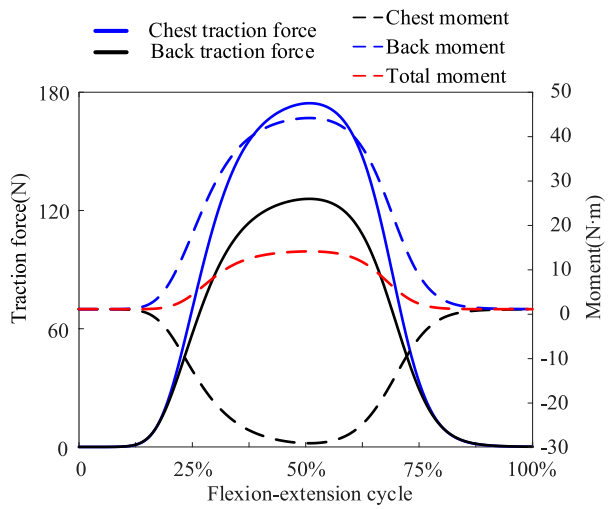

FIGURE 6
Based on the traction mechanics model, chest traction and back traction were calculated. Chest traction force produces an extension moment, back traction force produces a flexion moment, and a portion of both moments cancel out, creating a lower total extension moment provided by the exoskeleton.

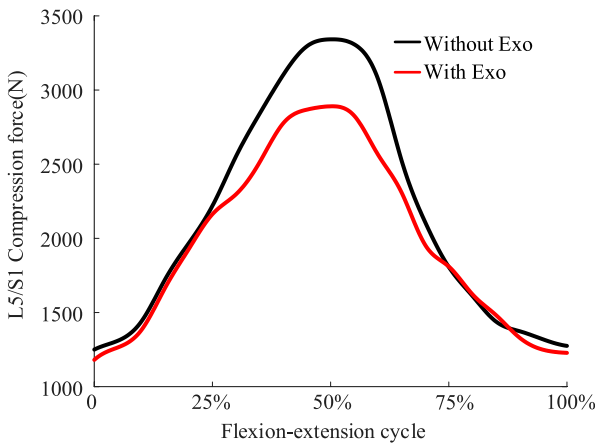

FIGURE 7
Comparison of disc compression forces at the L5/S1 joints before and after wearing the exoskeleton under an extreme load of 8 kg.

norm, causing a supervisor to observe the subject's posture in real time and to remind and correct his movements, using a metronome to control the tempo of the task. Subjects were made to not bend their knees and ankles as much as possible. If the knee and ankle flexion angles exceeded a certain threshold, the data from this set of experiments were nullified. This is because if the knee and ankle joints were overflexed it would affect the phenomenon of flexion relaxation (Shin et al., 2004),and would not be conducive to the observation of the connection between the exoskeleton and the EMG signals. All experimental situations were repeated six times, and after completing one set of experiments, the subjects were allowed to take a full rest for 10 min to prevent muscle fatigue.

3.3 Data processing

The original EMG signals were first imported into MATLAB, and the raw data were filtered using a fourth order Butterworth bandpass filter. Afterwards, the data were subjected to full-wave rectification and the RMS values of the EMG data were plotted. To ensure the comparability of electromyography (EMG) data among different subjects, the EMG signal data were normalized. Prior to the experimental tasks, the maximum voluntary contraction (MVC) of each subject was measured using the manual resistance method on a Roman chair (Biviá-Roig et al., 2019). The experimental signal values of each group were divided by the MVC signal values to obtain the normalized data, expressed as MVC%. This normalization allows signals from different individuals or different experimental conditions to be adjusted to the same scale, enabling direct comparisons between signals from different datasets or conditions and facilitating subsequent processing and analysis steps. The Kolmogorov - Smirnov test was employed to examine the normality of the electromyography (EMG) signal parameters. Subsequently, a paired t - test ($\alpha = 0.05$) was utilized to evaluate whether there were significant differences in the peak values of the MVC% signals before and after wearing the exoskeleton.

4 Results

4.1 Effects of traction force on spinal loading

Simulation results showed that the total stiffness of the optimized spring under 8 kg load was 1233 N/m. The chest and back traction provided by the exoskeleton increased with increasing flexion (Figure 6). The exoskeleton provided almost no traction and moment at the 0%–15% and 85%–100% stages. This is because at this stage the lumbar joints are less than 22.1°, the hip joints are less than 14.2°, and the angle of inclination of the human trunk is small enough that no more traction or extension moments are required. The exoskeleton provided maximum traction when the body reached 50% of the final stage of flexion, with thoracic traction of 173.4 N and dorsal traction of 125.5 N. The flexion moment generated by the dorsal traction partially offset the extension moment generated by the thoracic traction, making the overall extension moment generated by the exoskeleton appear not to be excessive (Figure 6). At the point where the body reaches 50% of the final stage of flexion, the maximum extension moment is just 13.1 N m. Lower support torque and higher traction performance may be better adapted in workplaces oriented to bending up under light loads or 0 kg loads (Zhang et al., 2023). Multiple traction forces demonstrated an excellent mechanical effect of reducing disc pressure (Figure 7), with the main reduction reflected in the peak phase of disc pressure, where peak compression forces were reduced from 3,326.4 N to 2,873.2 N.

4.2 Effects on the erector spinae muscle

The exoskeleton assist mechanism met the expectations of the objective function planning. At 8 kg weightbearing, muscle

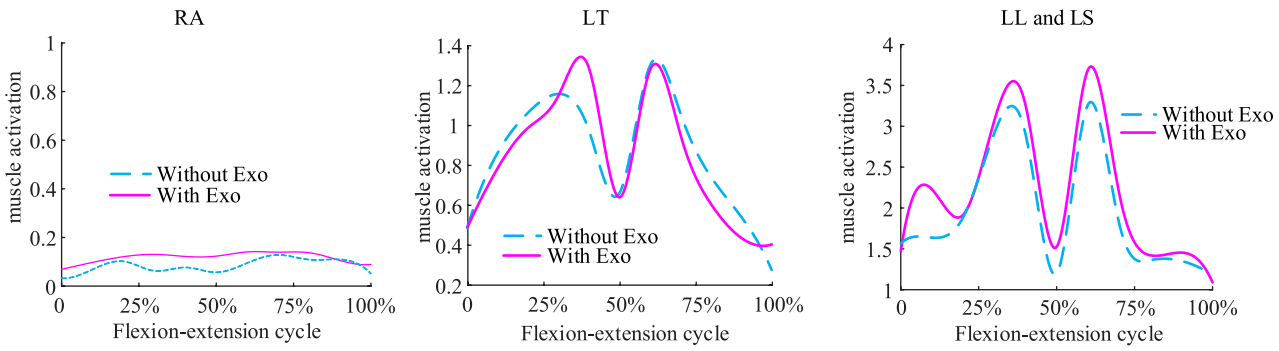

FIGURE 8
Comparison of muscle activation before and after wearing the exoskeleton under an extreme load of 8 kg. Muscle activation had a similar trend with or without wearing the exoskeleton.

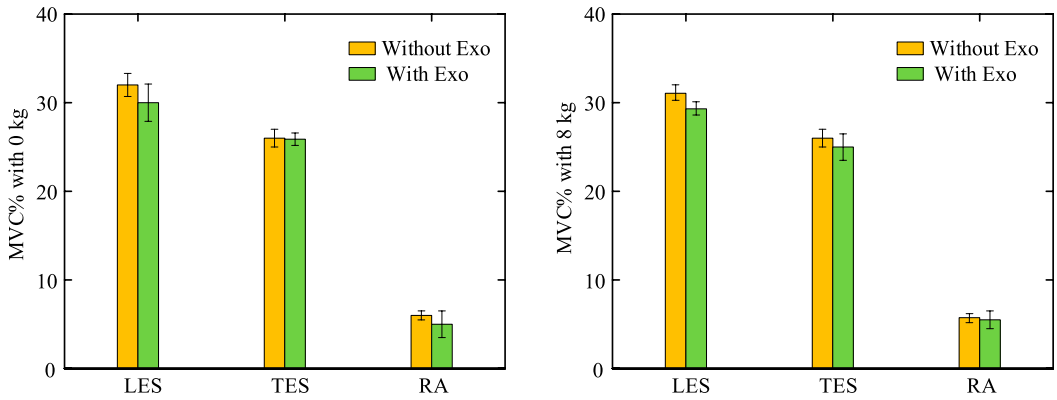

FIGURE 9
Percentage of peak EMG signals under dynamic bending and rising exercise. Comparative experiments with and without the exoskeleton were performed at 0 kg and 8 kg, confirming that the exoskeleton does not place an additional burden on the muscles.

activation before and after wearing the exoskeleton exhibited the following changes (Figure 8): during the 0%–25%, 50% and 75%–100% phases of the flexion-extension exercise cycle, which are phases in which the lumbar spine is in mild flexion or deep flexion, the muscle activation had a similar trend with or without wearing the exoskeleton, consistent with the lack of active muscle force during the flexion-relaxation phenomenon. Since the traction force of the exoskeleton can also generate a partial extension moment, a trend of reduced muscle activation after wearing the exoskeleton was observed during the partial flexion-extension movement interval. Simulation results showed that the activation of the rectus abdominis muscle did not change much before and after the subjects wore the exoskeleton, and never exceeded the upper limit of 0.2. The experimental results (Figure 9) showed that, in the 0 kg experimental group, there was no significant difference in the level of EMG signals in the thoracic erector spinae muscle after wearing the exoskeleton ($p = 0.62$). The peak EMG signals of both the lumbar erector spinae and rectus abdominis muscles were slightly reduced, by 6.41% in the lumbar erector spinae ($p = 0.036$) and by 18.08% in the rectus abdominis ($p = 0.02$). In the 8 kg experimental group, the level of electromyographic signals in the thoracic erector spinae muscle after wearing the exoskeleton was also not significantly different ($p = 0.226$). Both the lumbar erector spinae and rectus abdominis muscles also had a slight decrease in peak EMG signals, with the lumbar erector spinae decreasing by 7.32% ($p = 0.015$) and the rectus abdominis decreasing by 16.03% ($p = 0.023$). The peak EMG signal of the rectus abdominis was consistently much lower than that of the erector spinae in both the 0 kg and 8 kg experiments and no significant elevation of the peak EMG signal of the rectus abdominis was observed with the exoskeleton. Because of the low extension moments generated, the results of both simulations and experiments observed a low impact of the exoskeleton on the muscles, which is consistent with the original design intent that the traction generated by the exoskeleton is more focused on reducing disc pressure than on reducing muscle activation.

5 Discussion

This study introduces a novel passive lower back support exoskeleton, which leverages the principles of leverage to provide two types of traction forces. By sacrificing part of the chest traction force that generates extension torque, the exoskeleton incorporates a

lever mechanism to create back traction, achieving a lower support torque and a higher upper limit on traction force. A theoretical mechanics model of traction force supports this concept: as lumbar and hip flexion increases, intervertebral disc compression forces, along with both types of traction forces, also increase. Previous electromyographic studies have shown that passive exoskeleton-assisted extension moment reduces some active muscle forces, although this approach has a specific load threshold. Early designs of flexible exoskeletons or biomechanical garments have reduced muscle exertion to some extent, indirectly decreasing intervertebral disc loading. However, as the traction force ultimately acts on the spine, its effect on reducing disc pressure is limited. Some exoskeletons incorporate energy-storing components at the hip joint to support the torso, focusing on generating extension moment to reduce muscle force. However, this design overlooks the contribution of passive tissues, significantly limiting lumbar kinematics.

In practice, for light or zero-load bending and lifting movements, lumbar flexion rather than hip flexion is often the dominant motion pattern. Excessive extension moment generated by traditional exoskeletons can place an additional burden on the user. During trunk flexion-relaxation, the body ceases to engage active muscle forces, making moment demands on the exoskeleton more sensitive. If the exoskeleton's assistive moment exceeds a certain threshold, the user may need to compensate by other means, such as activating abdominal muscles to generate counteracting flexion moment or modifying movement patterns toward a squatting posture. Previous studies on passive back exoskeletons reported increased abdominal muscle activity, with forces from the erector spinae and rectus abdominis aligning in the direction of disc compression. The impact of this additional activation pattern on spinal stability remains highly debated. Ultimately, these studies concluded that reduced electromyographic signals do not necessarily indicate reduced spinal load, and the relationship between the two remains unclear, with potential concerns about spinal loading (Koopman et al., 2020a; Koopman et al., 2019). In basic industry, lumbar compression force is a critical measure of spinal injury risk, as it can lead to disc herniation, one of the most common lumbar disorders (Jaffar Nur and Abdol, 2017). Traction forces, moreover, have been proven to effectively reduce disc compression, with therapeutic traction reaching up to 500 N to achieve significant results in lumbar traction therapy (Zaïri et al., 2021). Thus, in workplaces where bending and lifting with light or zero loads is required—such as long-duration lumbar flexion for surgeons or crop harvesting for agricultural workers—lower support moment combined with higher traction may offer better adaptability. For such occupations, exoskeletons focusing on traction rather than assistive moment could be more advantageous. This forms the core feature of our exoskeleton design: sacrificing some extension moment to achieve higher traction, offering a new design perspective on lumbar exoskeletons tailored to occupational needs.

The lower back exoskeleton previously proposed by Chaerim Moon (Moon et al., 2022) employed a cross 4-bar linkage mechanism. However, due to the intrinsic properties of this mechanism, the efficiency of spring force transmission was low, necessitating a high spring stiffness to achieve the allowable standard for traction force. Furthermore, the relationship between the generated traction force and moment in this exoskeleton was not well-defined. In contrast, the dual traction forces in our exoskeleton design have minimal pressure angle deviations from the direction of intervertebral disc pressure, resulting in notably enhanced force transmission performance.

Additionally, considering the ligaments, intervertebral discs, and passive muscle forces, we set an overall traction force limit of 500 N (as higher traction could be harmful to the lumbar spine) (Zaïri et al., 2021). Optimal control was used to determine the optimal stiffness of the exoskeleton springs, thereby defining the traction force range. The optimization objective function aligns not only with the body's actual force generation patterns but also conforms to the original design of the exoskeleton to minimize the pressure on the L5/S1 disc. The simulation framework also provided predictions of intervertebral disc loading, which are difficult to measure in real experiments. The simulation results indicate that the optimized stiffness reduced the activation level of the erector spinae muscle group, and at maximum lumbar flexion, the peak compressive force on the intervertebral discs was effectively reduced.

The EMG shows that the optimized stiffness during the flexion and rise phases does not significantly increase abdominal muscle activity during the flexion and lifting phases, while activation of the thoracic longissimus and iliocostalis muscles decreased. This indicates that the extension moments generated by chest traction force is greater than the flexion moments generated by back traction force. This means that the extension moment produced by chest traction is greater than the flexion moment produced by back traction. The sum of the traction forces was also within the size range of effective traction forces and did not exceed the upper limit of more than 500 N. If the exoskeleton generated excessive extension moments, additional flexion moments are required to achieve moment equilibrium, and therefore, unintentional abdominal muscle activation may occur.

This study has several limitations. First, our prototype was designed as a rigid structure, with the assumption that the exoskeleton (made from lightweight materials) has zero mass, thereby neglecting the impact of inertial forces on the spring force and leverage. Second, our study was conducted solely in the sagittal plane, restricting lateral bending and rotation, and thus the effects of forces in other directions on intervertebral disc pressure remain unknown. Third, the connection between the exoskeleton and the human body was assumed to be fixed, but in reality, friction and damping coefficients between materials and the body may lead to relative slippage of the straps along the torso (Samper-Escudero et al., 2022), which could impact spring compression and the direction of traction force. Future research may need to establish a human-machine interaction model to predict the effects of such slippage, possibly by using materials with higher friction coefficients for the straps to minimize slippage. Fourth, the stiffness optimization was based on inverse dynamics; while this approach captures how stiffness affects muscle activation and disc pressure during standard movements, in reality, due to neurological reflexes, environmental factors, etc., exoskeletons may cause psychological or physiological burdens on the wearer and alter kinematics (Rimmele et al., 2023). In particular, the movement rhythm of the spine and spinal stability may change, which cannot be predicted by inverse dynamics. In the future, it is necessary to establish a forward dynamics model and make improvements based on the existing

musculoskeletal models. For example, modify the description of spinal movement rhythm and evaluate movement stability through the position of the center of pressure (CoP) within the support polygon (Shan et al., 2025). This approach can predict more information in the absence of experimental data (Jin et al., 2024). Finally, the experimental subjects were limited to healthy young males and the experimental period was relatively short. If the diversity of subjects can be realized and the experimental period can be lengthened, it will be helpful to reveal the adaptability of exoskeletons to the general population and to consider muscle fatigue and ligament viscoelasticity in subjects wearing exoskeletons for a long period of time (Ojha et al., 2024).

6 Conclusion

In this study, we developed an exoskeleton that provides two types of traction forces using a single spring. The exoskeleton was designed for work environments involving light load lifting and bending, as well as addressing the compressive characteristics of spinal pressure during flexion relaxation. Its novelty lies in the use of a lever mechanism to sacrifice moment in exchange for additional traction force, resulting in lower moment support and higher traction force. Consequently, it demonstrates exceptional performance in reducing intervertebral disc pressure without compromising active muscle force generation. The traction force model estimates the trends of the two forces. Optimal traction force ranges were determined through stiffness optimization, and reductions in intervertebral disc pressure peaks and cumulative loads were estimated. Electromyography results indicate that wearing this exoskeleton reduces active muscle force, potentially alleviating lower back pain caused by prolonged or repetitive bending and lifting. Future work will focus on lightweight design considerations to ensure both wearer comfort and the mechanical reliability of the exoskeletons.

Data availability statement

The raw data supporting the conclusions of this article will be made available by the authors, without undue reservation.

Ethics statement

The studies involving humans were approved by The Ethical Review Committee of Hebei University of Technology. The studies were conducted in accordance with the local legislation and institutional requirements. The participants provided their written informed consent to participate in this study. Written informed consent was obtained from the individual(s) for the publication of any potentially identifiable images or data included in this article.

Author contributions

KQ: Data curation, Funding acquisition, Writing–review and editing. ZY: Data curation, Writing–original draft, Writing–review and editing. CL: Writing–review and editing. JZ: Writing–review and editing. JS: Writing–review and editing.

Funding

The author(s) declare that financial support was received for the research, authorship, and/or publication of this article. This work was funding by Central Guided Local Science and Technology Development Funding Program (Grant No. 236Z1814G).

Conflict of interest

The authors declare that the research was conducted in the absence of any commercial or financial relationships that could be construed as a potential conflict of interest.

Generative AI statement

The author(s) declare that no Generative AI was used in the creation of this manuscript.

Publisher's note

All claims expressed in this article are solely those of the authors and do not necessarily represent those of their affiliated organizations, or those of the publisher, the editors and the reviewers. Any product that may be evaluated in this article, or claim that may be made by its manufacturer, is not guaranteed or endorsed by the publisher.

References

Abdoli-E, M., Agnew, M. J., and Stevenson, J. M. (2006). An on-body personal lift augmentation device (PLAD) reduces EMG amplitude of erector spinae during lifting tasks. *Clin. Biomech.* 21, 456–465. doi:10.1016/j.clinbiomech.2005.12.021

Abdoli-E, M., and Stevenson, J. M. (2008). The effect of on-body lift assistive device on the lumbar 3D dynamic moments and EMG during asymmetric freestyle lifting. *Clin. Biomech.* 23, 372–380. doi:10.1016/j.clinbiomech.2007.10.012

Abdoli-Eramaki, M., Stevenson, J. M., Reid, S. A., and Bryant, T. J. (2007). Mathematical and empirical proof of principle for an on-body personal lift augmentation device (PLAD). *J. Biomechanics* 40, 1694–1700. doi:10.1016/j.jbiomech.2006.09.006

Ali, A., Fontanari, V., Schmoelz, W., and Agrawal, S. K. (2021). Systematic review of back-support exoskeletons and soft robotic suits. *Front. Bioeng. Biotechnol.* 9, 765257. doi:10.3389/fbioe.2021.765257

Bazrgari, B., Shirazi-Adl, A., and Arjmand, N. (2007). Analysis of squat and stoop dynamic liftings: muscle forces and internal spinal loads. *Eur. Spine J.* 16, 687–699. doi:10.1007/s00586-006-0240-7

Biviá-Roig, G., LisóN, J. F., and SáNCHEZ-Zuriaga, D. (2019). Determining the optimal maximal and submaximal voluntary contraction tests for normalizing the erector spinae muscles. *PeerJ* 7, e7824. doi:10.7717/peerj.7824

Brown, S. H., and Potvin, J. R. (2005). Constraining spine stability levels in an optimization model leads to the prediction of trunk muscle cocontraction and improved spine compression force estimates. *J. Biomechanics* 38, 745–754. doi:10.1016/j.jbiomech.2004.05.011

Carnegie, D. R., Zehr, J. D., Howarth, S. J., and Beach, T. A. (2022). Kinematic adaptations to restricting spine motion during symmetrical lifting. *J. Electromyogr. Kinesiol.* 67, 102716. doi:10.1016/j.jelekin.2022.102716

Chow, D. H., Yuen, E. M., Xiao, L., and Leung, M. C. (2017). Mechanical effects of traction on lumbar intervertebral discs: a magnetic resonance imaging study. *Musculoskelet. Sci. Pract.* 29, 78–83. doi:10.1016/j.msksp.2017.03.007

Colloca, C. J., and Hinrichs, R. N. (2005). The biomechanical and clinical significance of the lumbar erector spinae flexion-relaxation phenomenon: a review of literature. *J. Manip. physiological Ther.* 28, 623–631. doi:10.1016/j.jmpt.2005.08.005

ConsmüLLER, T., Rohlmann, A., Weinland, D., Druschel, C., Duda, G. N., and Taylor, W. R. (2012). Comparative evaluation of a novel measurement tool to assess lumbar spine posture and range of motion. *Eur. spine J.* 21, 2170–2180. doi:10.1007/s00586-012-2312-1

Deb, K. (1999). Multi-objective genetic algorithms: problem difficulties and construction of test problems. *Evol. Comput.* 7, 205–230. doi:10.1162/evco.1999.7.3.205

DE Groote, F., Kinney, A. L., Rao, A. V., and Fregly, B. J. (2016). Evaluation of direct collocation optimal control problem formulations for solving the muscle redundancy problem. *Ann. Biomed. Eng.* 44, 2922–2936. doi:10.1007/s10439-016-1591-9

DE Looze, M. P., Bosch, T., Krause, F., Stadler, K. S., and O'Sullivan, L. W. (2016). Exoskeletons for industrial application and their potential effects on physical work load. *Ergonomics* 59, 671–681. doi:10.1080/00140139.2015.1081988

D'Errico, A., Viotti, S., Baratti, A., Mottura, B., Barocelli, A. P., Tagna, M., et al. (2013). Low back pain and associated presenteeism among hospital nursing staff. *J. Occup. health* 55, 276–283. doi:10.1539/joh.12-0261-oa

Eskandari, A. H., Ghezelbash, F., Shirazi-Adl, A., Arjmand, N., and LarivièRE, C. (2025). Effect of a back-support exoskeleton on internal forces and lumbar spine stability during low load lifting task. *Appl. Ergon.* 123, 104407–104418. doi:10.1016/j.apergo.2024.104407

Fathallah, F. A. (2010). Musculoskeletal disorders in labor-intensive agriculture. *Appl. Ergon.* 41, 738–743. doi:10.1016/j.apergo.2010.03.003

Fethke, N. B., Merlino, L. A., Gerr, F., Schall, J. R. M. C., and Branch, C. A. (2015). Musculoskeletal pain among Midwest farmers and associations with agricultural activities. *Am. J. industrial Med.* 58, 319–330. doi:10.1002/ajim.22398

Friedrich, M., Cermak, T., and Heiller, I. (2000). Spinal troubles in sewage workers: epidemiological data and work disability due to low back pain. *Int. archives Occup. Environ. health* 73, 245–254. doi:10.1007/s004200050424

Frost, D. M., Abdoli-E, M., and Stevenson, J. M. (2009). PLAD (personal lift assistive device) stiffness affects the lumbar flexion/extension moment and the posterior chain EMG during symmetrical lifting tasks. *J. Electromyogr. Kinesiol.* 19, e403–e412. doi:10.1016/j.jelekin.2008.12.002

Govaerts, R., DE Bock, S., Provyn, S., Vanderborght, B., Roelands, B., Meeusen, R., et al. (2024). The impact of an active and passive industrial back exoskeleton on functional performance. *Ergonomics* 67, 597–618. doi:10.1080/00140139.2023.2236817

He, W., Li, J.-L., Wang, J.-Y., He, D., and Song, K. (2024). Optimization of traction parameters for lumbar scoliosis. *BMC Musculoskelet. Disord.* 25, 472. doi:10.1186/s12891-024-07583-y

Hwang, J., Yerriboina, V. N. K., Ari, H., and Kim, J. H. (2021). Effects of passive back-support exoskeletons on physical demands and usability during patient transfer tasks. *Appl. Ergon.* 93, 103373. doi:10.1016/j.apergo.2021.103373

Jaffar Nur, A. T., and Abdol, R. M. N. (2017). Review on risk factors related to lower back disorders at workplace. IOP Conference Series. *Mater. Sci. Eng.* 226, 012035. doi:10.1088/1757-899X/226/1/012035

Jin, W., Liu, J., Zhang, Q., Zhang, X., Wang, Q., Xu, J., et al. (2024). Forward dynamics simulation of a simplified neuromuscular-skeletal-exoskeletal model based on the CMA-ES optimization algorithm: framework and case studies. *Multibody Syst. Dyn.* 62, 525–558. doi:10.1007/s11044-024-09982-4

Keawduangdee, P., Puntumetakul, R., Chatchawan, U., Kaber, D., and Siritaratiwat, W. (2012). Prevalence and associated risk factors of low-back pain in textile fishing net manufacturing. *Hum. Factors Ergonomics Manuf. and Serv. Industries* 22, 562–570. doi:10.1002/hfm.20375

Koopman, A. S., Kingma, I., DE Looze, M. P., and VAN DieëN, J. H. (2020a). Effects of a passive back exoskeleton on the mechanical loading of the low-back during symmetric lifting. *J. biomechanics* 102, 109486. doi:10.1016/j.jbiomech.2019.109486

Koopman, A. S., Kingma, I., Faber, G. S., DE Looze, M. P., and VAN DieëN, J. H. (2019). Effects of a passive exoskeleton on the mechanical loading of the low back in static holding tasks. *J. biomechanics* 83, 97–103. doi:10.1016/j.jbiomech.2018.11.033

Koopman, A. S., NäF, M., Baltrusch, S. J., Kingma, I., Rodriguez-Guerrero, C., Babič, J., et al. (2020b). Biomechanical evaluation of a new passive back support exoskeleton. *J. Biomechanics* 105, 109795. doi:10.1016/j.jbiomech.2020.109795

Kranenborg, S., Greve, C., Reneman, M., and Roossien, C. (2023). Side-effects and adverse events of a shoulder-and back-support exoskeleton in workers: a systematic review. *Appl. Ergon.* 111, 104042. doi:10.1016/j.apergo.2023.104042

Kuo, C.-S., Hu, H.-T., Lin, R.-M., Huang, K.-Y., Lin, P.-C., Zhong, Z.-C., et al. (2010). Biomechanical analysis of the lumbar spine on facet joint force and intradiscal pressure-a finite element study. *BMC Musculoskelet. Disord.* 11, 151–213. doi:10.1186/1471-2474-11-151

Lamers, E. P., Yang, A. J., and Zelik, K. E. (2017). Feasibility of a biomechanically-assistive garment to reduce low back loading during leaning and lifting. *IEEE Trans. Biomed. Eng.* 65, 1674–1680. doi:10.1109/tbme.2017.2761455

Luger, T., BäR, M., Seibt, R., Rieger, M. A., and Steinhilber, B. (2023). Using a back exoskeleton during industrial and functional tasks—effects on muscle activity, posture, performance, usability, and wearer discomfort in a laboratory trial. *Hum. Factors* 65, 5–21. doi:10.1177/00187208211007267

Madinei, S., and Nussbaum, M. A. (2023). Estimating lumbar spine loading when using back-support exoskeletons in lifting tasks. *J. Biomechanics* 147, 111439. doi:10.1016/j.jbiomech.2023.111439

Manns, P., Sreenivasa, M., Millard, M., and Mombaur, K. (2017). Motion optimization and parameter identification for a human and lower back exoskeleton model. *IEEE Robotics Automation Lett.* 2, 1564–1570. doi:10.1109/lra.2017.2676355

Mcgill, S. M., and Kippers, V. (1994). Transfer of loads between lumbar tissues during the flexion-relaxation phenomenon. *Spine* 19, 2190–2196. doi:10.1097/00007632-199410000-00013

Millard, M., Uchida, T., Seth, A., and Delp, S. L. (2013). Flexing computational muscle: modeling and simulation of musculotendon dynamics. *J. biomechanical Eng.* 135, 021005. doi:10.1115/1.4023390

Moon, C., Bae, J., Kwak, J., and Hong, D. (2022). A lower-back exoskeleton with a four-bar linkage structure for providing extensor moment and lumbar traction force. *IEEE Trans. Neural Syst. Rehabilitation Eng.* 30, 729–737. doi:10.1109/tnsre.2022.3159178

Moya-Esteban, A., Durandau, G., VAN DER Kooij, H., and Sartori, M. (2023). Real-time lumbosacral joint loading estimation in exoskeleton-assisted lifting conditions via electromyography-driven musculoskeletal models. *J. biomechanics* 157, 111727. doi:10.1016/j.jbiomech.2023.111727

NäF, M. B., Koopman, A. S., Baltrusch, S., Rodriguez-Guerrero, C., Vanderborght, B., and Lefeber, D. (2018). Passive back support exoskeleton improves range of motion using flexible beams. *Front. Robotics AI* 5, 72. doi:10.3389/frobt.2018.00072

Naserkhaki, S., Arjmand, N., Shirazi-Adl, A., Farahmand, F., and EL-Rich, M. (2018). Effects of eight different ligament property datasets on biomechanics of a lumbar L4-L5 finite element model. *J. biomechanics* 70, 33–42. doi:10.1016/j.jbiomech.2017.05.003

Ojha, A., Gautam, Y., Jebelli, H., and Akanmu, A. (2024). Physiological impact of powered back-support exoskeletons in construction: analyzing muscle fatigue, metabolic cost, ergonomic risks, and stability. *Automation Constr.* 168, 105742. doi:10.1016/j.autcon.2024.105742

Ostraich, B., and Riemer, R. (2024). Rethinking exoskeleton simulation-based design: the effect of using different cost functions. *IEEE Trans. Neural Syst. Rehabilitation Eng.* 32, 2153–2164. doi:10.1109/tnsre.2024.3409633

Pal, P., Milosavljevic, S., Sole, G., and Johnson, G. (2007). Hip and lumbar continuous motion characteristics during flexion and return in young healthy males. *Eur. Spine J.* 16, 741–747. doi:10.1007/s00586-006-0200-2

Pearsall, D. J., Reid, J. G., and Livingston, L. A. (1996). Segmental inertial parameters of the human trunk as determined from computed tomography. *Ann. Biomed. Eng.* 24, 198–210. doi:10.1007/bf02667349

Pellecchia, G. L. (1994). Lumbar traction: a review of the literature. *J. Orthop. and Sports Phys. Ther.* 20, 262–267. doi:10.2519/jospt.1994.20.5.262

Picchiotti, M. T., Weston, E. B., Knapik, G. G., Dufour, J. S., and Marras, W. S. (2019). Impact of two postural assist exoskeletons on biomechanical loading of the lumbar spine. *Appl. Ergon.* 75, 1–7. doi:10.1016/j.apergo.2018.09.006

Pintar, F. A., Yoganandan, N., Myers, T., Elhagediab, A., and Sances, J. R. A. (1992). Biomechanical properties of human lumbar spine ligaments. *J. biomechanics* 25, 1351–1356. doi:10.1016/0021-9290(92)90290-h

Poliero, T., Fanti, V., Sposito, M., Caldwell, D. G., and DI Natali, C. (2022). Active and passive back-support exoskeletons: a comparison in static and dynamic tasks. *IEEE Robotics Automation Lett.* 7, 8463–8470. doi:10.1109/lra.2022.3188439

Rahmati, M., Rostami, M., and Beigzadeh, B. (2017). A low-cost optimization framework to solve muscle redundancy problem. *Nonlinear Dyn.* 90, 2277–2291. doi:10.1007/s11071-017-3802-9

Rimmele, P., Steinhilber, B., Rieger, M. A., and Luger, T. (2023). Motor variability during a repetitive lifting task is impaired by wearing a passive back-support exoskeleton. *J. Electromyogr. Kinesiol.* 68, 102739. doi:10.1016/j.jelekin.2022.102739

Samper-Escudero, J. L., Coloma, S., Olivares-Mendez, M. A., Gonzalez, M. A. S.-U., and Ferre, M. (2022). A compact and portable exoskeleton for shoulder and elbow assistance for workers and prospective use in space. *IEEE Trans. Human-Machine Syst.* 53, 668–677. doi:10.1109/thms.2022.3186874

Senteler, M., Weisse, B., Rothenfluh, D. A., and Snedeker, J. G. (2016). Intervertebral reaction force prediction using an enhanced assembly of OpenSim models. *Comput. methods biomechanics Biomed. Eng.* 19, 538–548. doi:10.1080/10255842.2015.1043906

Shan, M., Li, C., Sun, J., Xie, H., Qi, Y., Niu, W., et al. (2025). The trunk segmental motion complexity and balance performance in challenging seated perturbation among individuals with spinal cord injury. *J. NeuroEngineering Rehabilitation* 22, 4. doi:10.1186/s12984-024-01522-7

Shin, G., Shu, Y., Li, Z., Jiang, Z., and Mirka, G. (2004). Influence of knee angle and individual flexibility on the flexion–relaxation response of the low back musculature. *J. Electromyogr. Kinesiol.* 14, 485–494. doi:10.1016/s1050-6411(03)00153-6

Solomonow, M., Baratta, R. V., Banks, A., Freudenberger, C., and Zhou, B. H. (2003). Flexion–relaxation response to static lumbar flexion in males and females. *Clin. Biomech.* 18, 273–279. doi:10.1016/s0268-0033(03)00024-x

Tadano, S., Tanabe, H., Arai, S., Fujino, K., Doi, T., and Akai, M. (2019). Lumbar mechanical traction: a biomechanical assessment of change at the lumbar spine. *BMC Musculoskelet. Disord.* 20, 155–212. doi:10.1186/s12891-019-2545-9

Toussaint, H. M., DE Winter, A. F., DE Haas, Y., DE Looze, M. P., VAN DieëN, J. H., and Kingma, I. (1995). Flexion relaxation during lifting: implications for torque production by muscle activity and tissue strain at the lumbo-sacral joint. *J. biomechanics* 28, 199–210. doi:10.1016/0021-9290(94)00051-5

Wong, K. W., Luk, K. D., Leong, J. C., Wong, S. F., and Wong, K. K. (2006). Continuous dynamic spinal motion analysis. *Spine* 31, 414–419. doi:10.1097/01.brs.0000199955.87517.82

ZaïRI, F., Moulart, M., Fontaine, C., ZaïRI, F., Tiffreau, V., and Logier, R. (2021). Relevance of a novel external dynamic distraction device for treating back pain. *Proc. Institution Mech. Eng. Part H J. Eng. Med.* 235, 264–272. doi:10.1177/0954411920971401

Zhang, C., Roossien, C. C., Verkerke, G. J., Houdijk, H., Hijmans, J. M., and Greve, C. (2023). Biomechanical load of neck and lumbar joints in open-surgery training. *Sensors* 23, 6974. doi:10.3390/s23156974